Article

Comparison of a Static Membrane Bioreactor Fouling Model for Wastewater Treatment with an Innovative Rotational Membrane Bioreactor Model with the Rotational Function Switched Off

Parneet Paul [1,*] and Franck Anderson [2]

[1] School of Built Environment and Engineering, Leeds Beckett University, Northern Terrace, Queen Square Court, Leeds, LS2 8AJ, United Kingdom; p.paul@leedsbeckett.ac.uk
[2] Department of Mechanical, Aerospace, and Civil Engineering, College of Engineering, Design and Physical Sciences, Brunel University, Uxbridge, Middlesex, UB8 3PH, United Kingdom; mepgfaj@brunel.ac.uk
* Correspondence: p.paul@leedsbeckett.ac.uk; Tel.: +44-(0)-113-812-8292

Featured Application: Static membrane bioreactor systems do perform well in wastewater treatment, but they might be supplanted in the future by newly developed rotating membrane bioreactor systems that potentially have both reduced bio-fouling and subsequent energy consumption. However, the current rotational simulation models that can be used for improved process control are in their early stages of development and validation when compared to their static counterparts.

Abstract: Fouling by activated sludge in membrane bioreactor (MBR) processes for wastewater treatment can be reduced using several strategies such as backflushing, relaxation, and chemical cleaning. Some proprietary systems such as Avanti's RPU-185 Flexidisks MBR use novel circular rotating, flat sheet membranes to assist in limiting this fouling. An attempt has already been made to model this novel rotating fouling process by developing a simulation model based on first principles and traditional fouling mechanisms. In order to directly compare the potential benefits of rotational MBR system, a follow-up study was carried out using Avanti's newly developed static (non-rotating) Flexidisks MBR system. This new process uses the same proprietary and patented membrane modular arrangement as used in the circular rotational unit, but is configured instead as a static square-shaped unit which is in-line with the more traditional and popular format used for submerged flat sheet MBR systems. During this study, the results from operating the static pilot unit were simulated and modelled using a standard fouling model coupled with a viscosity to mixed liquor relationship model. These results were then compared with those obtained from running the rotating MBR model however with rotational switching functions turned off and rotational parameters set to a static mode. This comparison was done to ascertain whether the basic premise of the developed rotational model was sound in empirical terms when compared to a standard MBR flux model. The study concluded that relatively good agreement was reached between the two types of models, thus vindicating the usage of a complex rotational MBR model. Follow on studies will now compare results from the rotating MBR system using rotational models developed by other researchers to ascertain the effectiveness rotating MBR modelling approach.

Keywords: membrane bioreactor (MBR); wastewater; rotating membranes; static membranes; fouling; modelling

1. Introduction

Water scarcity is a growing problem faced in a global context, with most regions of the world having nearly fully exploited all sources of water. Conversely, potentially "new" sources of water,

such as rainwater harvesting and wastewater reuse via recycling are ruthlessly underutilised at the moment [1]. Major drawbacks of the latter option, however, are disinfection of product to sufficient cleansed levels, and other ethical issues such as potable reuse of treated black water.

Undeniably, treatment of wastewater streams has been an increasingly daunting task facing engineers for many decades due to varying, complex influent characteristics and every, stringent effluent regulations. Although initial solutions to these issues involved the use of standalone biological wastewater treatment systems such as conventional activated sludge (CAS) processes, it quickly became apparent there were potential efficiency gains in process intensification. Furthermore, major setbacks were economics and land related. The practice of using CAS processes came at huge expense and involved large environmental footprints to achieve the desired effluent water quality, especially for medium to large wastewater treatment facilities [2,3].

A serious alternative to the usage of CAS processes came with the introduction of filtration technologies known as membrane bioreactors (MBRs), in particular non-rotating or static MBRs (SMBRs). Since their emergence, they have experienced a dramatic increase in usage over the past three decades, especially since they can be retrofitted to an existing CAS process [4,5].

A reason why they are so coveted is chiefly because they offer several advantages over CAS and other traditional wastewater treatment processes. Not only do they allow recycling but they also produce better effluent and permeate quality as well as significantly reduced footprints [6,5]. Furthermore, their practice is economically sound when compared to CAS [7]. Nowadays, they can also cope with large effluent quantities as well.

Although these SMBR systems do perform well, they might be supplanted in the future by newly developed rotating MBR (RMBR) systems that potentially have reduced bio-fouling and subsequent energy consumption [8]. RMBRs characteristically induce high shear effects on the membrane surface thereby reducing associated fouling whilst minimising energy usage. These systems have been shown to yield high permeate flux in the ultra-filtration (UF) range [9], whilst the very high shear rate simultaneously yields a good system performance by preventing cake formation and subsequent increased concentration polarisation [10,11].

Unfortunately, a single persistent issue, namely membrane fouling that is characterised by flux decline or trans-membrane pressure (TMP) increase during MBR filtration operation time, which has been bedevilling this field of research for years, came to light along with the increase usage of MBRs [12,13]. Fouling by non-Newtonian fluids such as activated sludge used in MBR systems is a key limiting factor in UF membrane processes.

The true origin of fouling has yet to be truly defined, although many researchers widely acknowledge that SMP (soluble microbial products) and EPS (extracellular polymeric substances) are the most likely fouling agents [12]. This is since the build-up of SMP and EPS can cause reduction in membrane permeability [14,15]. Additional factors affecting fouling mechanisms include: scaling; biofilm formation; operating conditions, such as pH; temperature and flow rates; and, solution properties such as particle size distribution [12].

According to Hermia [16], during constant pressure UF filtration, three major fouling mechanisms can occur. These are typically known as pore constriction, pore blocking (usually divided into either “complete” or “intermediate”) and cake filtration. The aforementioned fouling mechanisms describe the accumulation of particles, solutes, and colloids inside the membrane’s pores and on the membrane’s surface leading to a reduction in the diameter of open pores (i.e., pore constriction), an obstruction of the pores by particles larger than the membrane’s pore size (i.e., pore blockage) and the deposition of layers of particles onto the blocked membrane surface (i.e., cake filtration).

Moreover, depending on the composition of the liquid being filtered and the interactions between the membrane and the bulk liquid, one fouling process may dominate over the other two or all three mechanisms may simultaneously occur throughout the filtration’s duration time [16]. Many fouling studies have been carried out to date using pilot units in order to determine the best operating conditions of MBR systems, although currently, due to the complexity of the biomass matrix which includes living micro-organisms, no definitive theories on membrane fouling have

Preprints (www.preprints.org) | NOT PEER-REVIEWED | Posted: 12 June 2018 doi:10.20944/preprints201806.0187.v1

been established [6,17]. This situation is further exacerbated with the membranes themselves having being laid down as phase inverted anisotropic media, meaning the pores themselves are not uniform, following often very tortuous paths, with a very thin selective outer layer, and gradually increasing thickness of backing layer with large irregular inter-connected pore spaces between.

Different approaches have also been developed for modelling the physical and biological aspects of membrane fouling in a normal non-rotational MBR system. For instance Meng et al. [18], established a fractal permeation model while Liu et al. [19], presented an empirical hydrodynamic model. Duclos-Orsello et al. [20], introduced a fouling model that combined all three classical fouling mechanisms which was later used by Paul [21] as a starting point for a greatly refined model for a side-stream MBR that incorporated both hydrodynamics and SMP effects.

Because mathematical modelling can be used to simulate flux decline and thus potentially afford a greater understanding of the membrane fouling mechanisms involved, the aims of this study was to:

1. Create a new, comprehensive fouling model that incorporates hydrodynamic regimes for a standard SMBR using a viscosity to mixed liquor relationship model developed by Yang et al. [22]. Then validate said fouling model using filtration data collected from operating the Avanti's square-shaped SMBR.
2. Compare these results with those obtained from running the Paul and Jones [23] RMBR model however with rotational switching functions turned off and rotational parameters set to a static mode.

2. Methods and Materials

2.1. Theoretical Approach

Since the square-shaped SMBR system was operated under constant transmembrane pressure (TMP), both fouling models (static square-shaped and standard) must be evaluated in terms of the varying flux. With this MBR mode of operation, as the filtration process goes on, the flux declines, indicating fouling.

In this research work, three fouling mechanisms are chosen. Let us consider Figure 1a), b) and c) as the fouling mechanisms that occur during a typical filtration process (e.g. UF) for membranes that have been fouled for the square-shaped SMBR. During the filtration timeline, fouling is observed with respect to the change in TMP (or flux), mixed liquor suspended solids (MLSS) level, or a combination of both.

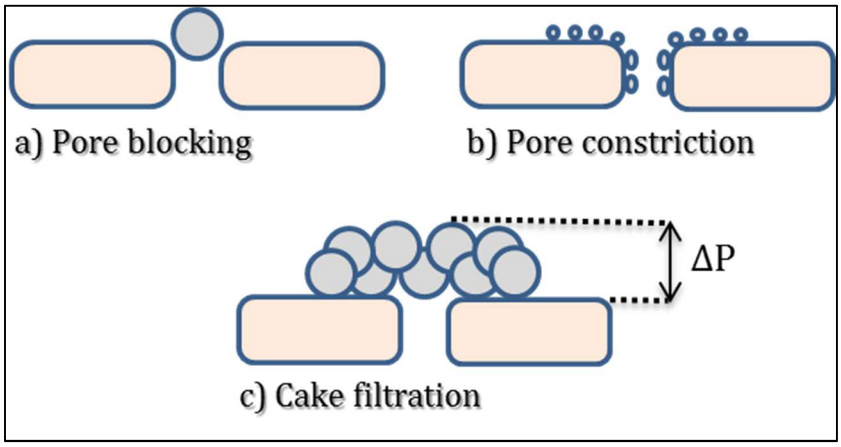

Figure 1. Diagram of the combined fouling mechanisms: Colloids or small particles constrict the pores while larger particles block them, and accumulate to form a cake.

Firstly whilst referring to Figure 1a), b) and c), it was assumed that the membrane's pores were cylindrical and uniformly distributed throughout the membrane, so that fluid flow could be

Preprints (www.preprints.org) | NOT PEER-REVIEWED | Posted: 12 June 2018 doi:10.20944/preprints201806.0187.v1

described by Hagen-Poiseuille flow. Hence, pore constriction occurs through all open pores, and gradually the membrane surface becomes obstructed by aggregates forming a somewhat uneven blocked area. Once the pores are blocked by aggregates, pore constriction is stopped.

Consequently, a cake layer will form over any blocked area. The resistance of this deposit layer is time dependent with regions of greatest resistance delivering the smallest flux. However, in reality the actual membrane fouling process is extremely complex in nature with usually all effects simultaneously occurring. Nevertheless, to simplify the model the above assumptions are made as well as overlooking the effect of frictional forces and temperature [23,24].

2.1.1. Square-Shaped SMBR Fouling Model

Paul and Jones [23] developed a comprehensive fouling model for Avanti's circular RMBR (RPU-185 pilot unit). This model included all three classical fouling mechanisms as well as the hydrodynamics including the rotating shear effects [23].

A bespoke SMBR system that utilised Avanti's square-shaped membrane module was then fabricated at our laboratory. Paul and Jones [24] developed a static fouling model based on this system. To obtain this fouling model, the rotating functions in the RMBR fouling model were switched-off. By removing the rotational switching functions, the fouling model of the RMBR reverts to that of a submerged SMBR system (i.e., square-shaped) that now simply includes the air scouring term as hydrodynamic regime. This is shown through Equation 1, which computes the total flow rate through membrane [24], Q_t ($m^3.s^{-1}$);

$$Q_t(t) = \frac{A_{u_0}.J_0}{(1+\beta.Q_0.C_{MLSS}.t)^2}.e^{\left\{\frac{\alpha.J_0}{\beta.Q_0}.\left(\frac{1}{1+\beta.Q_0.C_{MLSS}.t}-1\right)\right\}} + \frac{-PT}{\mu.(R_m.(1+\beta.Q_0.C_{MLSS}.t_b)^2+R_b)}.\int_0^t\left(\frac{A_{u0}.\alpha.C_{MLSS}.J_0}{(1+\beta.Q_0.C_{MLSS}.t_b)^2}.e^{\left\{\frac{\alpha.J_0}{\beta.Q_0}.\left(\frac{1}{1+\beta.Q_0.C_{MLSS}.t_b}-1\right)\right\}}\right)dt_b \quad (1)$$

and, Equation 2, which includes hydrodynamic factor, air scouring flux, J_{air} ($m.s^{-1}$), to compute the net area effect [24].

$$\frac{dA_b}{dt} = \alpha.J_u.A_u.C_{MLSS} - k_{A_b}.(\alpha_v.J_{air}).\theta_c(t) \quad (2)$$

2.1.2. Standard SMBR Fouling Model

Activated sludge in MBR systems is classified as a non-Newtonian fluid that can be expressed as a function of MLSS. This was studied in depth in a study by Yang et al. [22]. From their study, viscosity (μ, Pa.s) is proportional to MLSS as seen in Equation 3 such that:

$$\mu = 0.0126.(C_{MLSS})^{1.664}.e^{\frac{E}{Rg.(Troom+273.15)}} \quad (3)$$

During UF, as the membrane becomes fouled and flux gradually decreases, the total available area for permeate will decrease at a uniform rate such that, there exist a time constant t_c (s^{-1}) < 1/t that yields area formulation Equation 4. Assuming time constant, t_c (s^{-1}), is proportional to the initial flux (as TMP is constant), the area formula Equation 4 can be further expanded such that:

$$A = A_0(1-t_c.t) = A_0(1-K_\alpha.Jm_0.t) \quad (4)$$

As can be observed from the above equation, it is quite similar to the Hermia [16] area formulation. A Taylor's expansion of order 1 of $\ln 1-K_\alpha.Jm_o.t$ at t = 0 is $\approx -K_\alpha.Jm_o.t$. This reduces the area formulation to Equation 5.

$$A = A_0.\ln\left(e.(1-K_\alpha.Jm_o.t)\right) \equiv A_0.e^{(-K_\alpha.Jm_o.t)} \quad (5)$$

Due to caking observed during UF process, the total resistance will increase with the membrane area available for filtration. According to the resistance-in-series approach, the total membrane resistance is defined as the summation of the cake's resistance and all other mechanisms' resistances.

Preprints (www.preprints.org) | NOT PEER-REVIEWED | Posted: 12 June 2018 doi:10.20944/preprints201806.0187.v1

As such, by including the pore constriction mechanism and constant φ, R_{total} (m^{-1}), can be can be computed as seen in Equation 6.

$$R_{total} = \left(R_{in,b} + \varphi . R_b\right) \quad (6)$$

At time t_b (s), once the pore constriction stops, the time at which a pore was first blocked, resistance $R_{in,b}$ can be calculated by Equation 7 [20].

$$R_{in,b} = R_m(1 + \beta . Q_0 . C_{MLSS} . t_b)^2 \quad (7)$$

The resistance of the particles deposit increases with time due to the growth in mass (or thickness) of the cake layer, and with the cake filtration model, resistance, R_b, (m^{-1}) is given by Equation 8.

$$\frac{dR_b}{dt} = f' . R' . J . C_{MLSS} \quad (8)$$

The flux, J ($m.s^{-1}$), can be calculated from Equation 9 using Darcy's law at constant TMP and the in-series resistance approach.

$$J = \frac{TMP}{\mu . \left(R_{in,b} + \varphi . R_b\right)} \quad (9)$$

Thus, by combining Equations 3 to 9, the total normalised flow rate through membrane, Q_t ($m^3.s^{-1}$), is expressed in Equation 10 as the product of the available area and the flux.

$$Q_t(t) = \frac{TMP}{0.0126 . (C_{MLSS})^{1.664} . e^{\frac{E}{R_g . (T_{room} + 273.15)}} . (R_m(1 + \beta . Q_0 . C_{MLSS} . t_b)^2 + \varphi . R_b)} . A_0 . e^{(-K_\alpha . Jm_0 . t)} \quad (10)$$

Where,

R_g is the universal gas constant (R_g = 8.3145 × 10^{-3} $kJ.K^{-1}.mol^{-1}$), E is the so-called activation energy which according to Yang et al. [22] is 9.217 ($kJ.mol^{-1}$) for the viscosity of sludge, T_{room} is the room temperature in °C.

The only prevalent hydrodynamic factor to take into account during operation of a standard submerged SMBR (e.g., bespoke square-shaped SMBR) is the air scouring which is mainly in charge of mitigating against cake growth and thus reduce fouling. Additionally, air scouring flux, J_{air} ($m.s^{-1}$), is a key parameter for the management and prevention of membrane fouling in most submerged MBR systems.

Thus, an additional removal term defined as the flux induced by the air scouring flow effects was added. This supplementary removal term is also in-line with Liang et al. [25], cake's formulation equation. An analogous reformulation is found in Equation 11 but includes the air scouring effects.

$$\frac{dR_b}{dt} = f' . R' . J . C_{MLSS} - g_o . (\alpha_v . J_{air}) . \delta' . (R'_c . \theta_c) \quad (11)$$

2.2. Materials

This section covers experimental procedures as well as the materials used to acquire the filtration data used in the model simulations.

2.2.1. SMBR plant set-up

Figure 2 shows the set-up and operation of the square-shaped SMBR rig that was fabricated at Brunel University using a bespoke static square-shaped membrane module (Flexidisks by Avanti Membrane Technology, Walnut, California, USA). This rig generated filtration data that in turn were used to validate and test the SMBR fouling models described in Section 2.1.

Preprints (www.preprints.org) | NOT PEER-REVIEWED | Posted: 12 June 2018 doi:10.20944/preprints201806.0187.v1

Figure 2. Static square-shaped membrane bioreactor (MBR) system in operation in the laboratory. The square membrane module is located in the larger tank on the right for filtration purposes.

The UF membrane module (as shown on Figure 3) consisted of 20 static membrane flat sheets. Each membrane sheet in square form was composed of hydrophilic, low fouling polyvinylidene fluoride (PVDF) polymer with the manifold that collected the permeate flow being located in the single shaft.

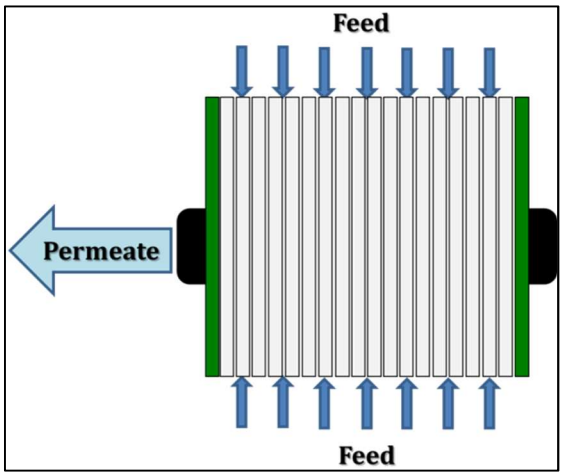

Figure 3. Schematic of static square-shaped membrane module that is located within the SMBR's batch tank.

The viscosity of the fluid was measured daily by the aid of rotating viscometers (Rotary-Viscometer ASTM by PCE Instruments UK Ltd, Southampton, UK; and High Shear CAP-2000+ by Brookfield Viscometers Ltd, Essex, UK), whilst the MLSS concentration was logged continuously by a MLSS analyser (GE-138 MLSS Suspended Solids Sludge Concentration Meter Analyser Monitor by A. Yite Technology Group, Wanchai, Hong Kong).

Table 1 shows this second unit's membrane dimensioning and a general overview of the operating conditions of the bespoke SMBR system as provided by the manufacturer.

Table 1. Dimensions of membrane module and operating conditions of the bespoke SMBR.

Description	Unit	Values
Individual Membrane Width	m	0.24
Individual Membrane Length	m	0.24
Total Membrane area	m^2	1.152
Operating Temperature	°C	~ 5 – 60 °C
Permeate flux	$L.m^2.h^{-1}$	> 30
TSS (Total Suspended Solids)	$g.L^{-1}$	> 8

Preprints (www.preprints.org) | NOT PEER-REVIEWED | Posted: 12 June 2018 doi:10.20944/preprints201806.0187.v1

TMP*	bar	> 3

* = Transmembrane Pressure

2.2.2. Plant Operational Regime

The SMBR plant was initially seeded with activated sludge supplied by Thames Water, UK, and were semi-batch fed a synthetic wastewater made up using a standard recipe to mimic an influent wastewater source. MLSS concentrations were kept between the range of 6.32 and 7.24 g/L by periodic excess sludge wasting. The influents had an average pH between the range of 7.8 and 8.6, and experiments were carried out at a constant room temperature of 23 °C.

2.2.3. TMP Stepping Experimentation

Using standard protocols in-line with Le Clech et al. [26] and Paul and Jones [23], TMP stepping was performed so as to procure filtration data from the bespoke SMBR. Although two TMP steps up were carried out for each variation in MLSS concentration, for validation of both models only one TMP step was considered: the high constant TMP of 45 kPa. Since biological activities occurring at this high TMP and MLSS levels are active, the probable irregularities in filtration data would be good to test the validity of both models. TMP steps were carried out at constant TMP of 15 kPa and TMP of 45 kPa.

The corresponding initial flow rates were respectively 1.2 x 10-5 m^3/s and 2.5 x 10-5 m^3/s. Although data was constantly being logged, for the sake of simplicity and to keep model computation time down to a minimum, only the average data points for every 5 minutes of filtration time were actually used in the simulation study with the total filtration period being two hours. This meant a total of 25 data points were generated for each individual MLSS concentration. After each TMP step testing, a chemical backwash was carried out with 125 mg/L worth of sodium hypochlorite solution and the membrane resistance was calculated to measure the extent of irreversible fouling.

On unit start-up, for the square-shaped SMBR system, the clean membrane resistance was determined to be 4.55 x 1011 m^{-1}.

3. Results and Discussions

The flow regimes during the filtration processes of the square-shaped SMBR were laminar which were well within expectations since calculated radial Reynolds number (R_{eNN}) values were much less than 2×10^5.

In the square-shaped SMBR fouling model, parameter α solely contributed to pore blocking, parameter β solely contributed to pore constriction and a combination of parameters $f'.R'$, R_{bo}, g_o and k_{Ab}, all contributed to cake filtration. For the standard SMBR model, parameter β contributed to pore constriction whilst a combination of parameters $f'.R'$, R_{bo} and g_o, all contributed to cake filtration. $K\alpha$ and φ were indicative terms for pore blocking.

The aeration rate for all the data sets for the SMBR system was similar in scale to that of the RMBR system operated under lab scale conditions (i.e., the usual air scouring flow rate of 3.55×10^{-4} m^3/s). Thus, similar constant values for air scouring coefficient, α_v, (i.e. 0.0292), and the resistance distribution factor of cake layer, δ', (i.e. 4.6×10^{-4} m^{-1}) were used during all simulations. So as to ascertain validity of both SMBR models, only the six most important parameters pertaining to the three fouling mechanisms were used for data and curve fitting during simulations.

These were $f'.R'$, α, β, R_{bo}/R_m, g_o and k_{Ab} for the square-shaped SMBR model and $f'.R'$, β, R_{bo}/R_m, g_o, K_α and φ for the standard SMBR model. For both fouling models, these best fit simulation values were attained by minimising the sum of squared residuals between the model and the collected experimental data. This was used in conjunction with "Genetic Algorithm" function in the Matlab software package with an initial population large enough for the data set used to converge to the minimal possible error. The simulations were performed for TMP of 45 kPa for MLSS concentration range of 6.32 g/L – 7.24 g/L. The simulations best fits parameters that were obtained are summarised in Table 2.

Preprints (www.preprints.org) | NOT PEER-REVIEWED | Posted: 12 June 2018 doi:10.20944/preprints201806.0187.v1

Table 2. Simulations best fit model parameters including hydrodynamic effects.

	Bespoke SMBR model	**Standard SMBR model using Yang et al. [22] viscosity model**
Optimised parameters	*Data simulated at TMP of 45 kPa and MLSS level range 6.32 g/L – 7.24 g/L*	
f'R' (m/kg)	108.8×10^{11}	106.9×10^{11}
α (m^2/kg)	0.907	–
β (*kg*)	0.486	0.637
R_{bo}/R_m (–)	0.526	0.466
g_o (–)	15.36	12.20
k_{Ab} (–)	14.23	–
Kα (m^{-1})	–	13.91
φ (–)	–	19.78

The obtained best fit values (Table 2) appear fairly sensible since they are in-line with earlier work done [24]. In addition, they also present an accurate depiction of the dominant fouling mechanisms. However, at this high TMP and MLSS concentration range, point-to-point simulations of experimental data of both models were quite poor (as seen later in Figure 4 and 5). A reason for this largely expected outcome is that sludge rhealogical effects which themselves are volatile will dominate nearly all membrane fouling mechanisms in unpredictable ways especially at high MLSS concentrations with associated high viscosities. This situation is less prevalent for the rotating MBR system, as both air scouring and rotational shear contribute to the reduction in fouling [23,24].

As part of the simulation process, curve fitting for the fouling decline of both SMBR systems were run in Matlab. Outputted results are shown in Figure 4 and 5 respectively.

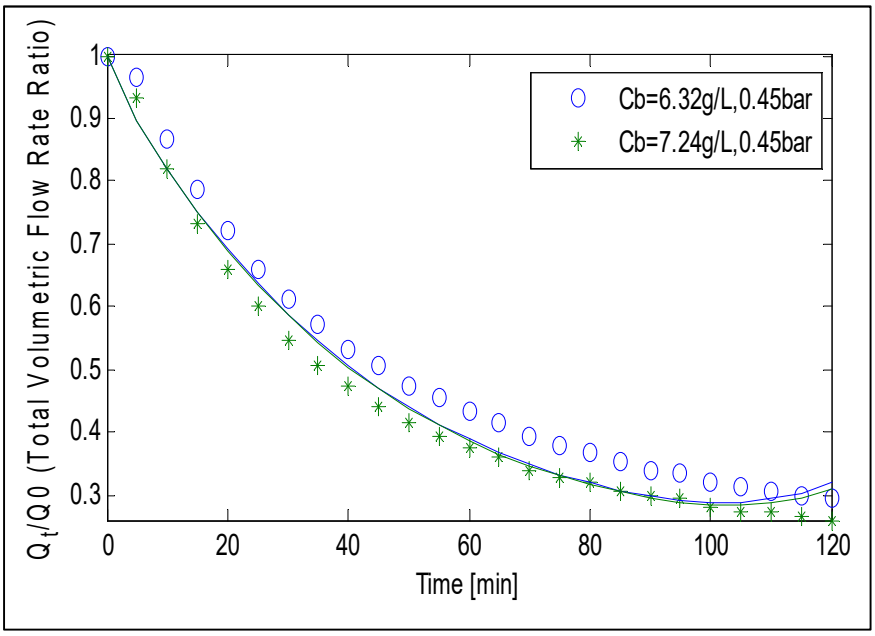

Figure 4. Standard SMBR model: Flux decline for TMP step at constant TMP of 45 kPa for MLSS concentration range 6.32 g/L – 7.24 g/L.

Preprints (www.preprints.org) | NOT PEER-REVIEWED | Posted: 12 June 2018 doi:10.20944/preprints201806.0187.v1

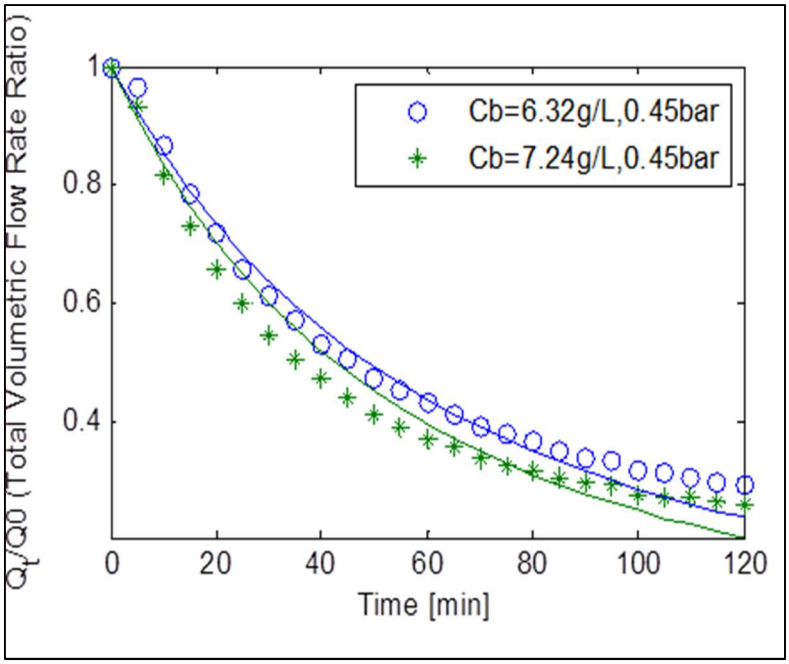

Figure 5. Bespoke SMBR model: Flux decline for TMP step at constant TMP of 45 kPa for MLSS concentration range 6.32 g/L – 7.24 g/L.

Figure 4 depicts the effects of the fouling behaviour of the standard SMBR model, using the normalised volumetric flow rates for MLSS concentrations of 6.32 and 7.24 g/L at a constant TMP of 45 kPa; with the solid lines representing the best fit simulation solutions. The experimental data show that there is massive flux decline. In fact, there is an over 70% drop in flux. At high MLSS levels biological activities tend to be extremely active, this means that flux will diminish at a faster rate (i.e., fouling occurring faster).

Therefore, this flux drop that is translated from the simulated fouling curve is well within expected margins of error [23]. Another obvious fact is that the point-to-point fit of experimental data is very poor. But, the fouling curve's trend is of the right magnitude and in the right direction to allow an analysis of the fouling behaviour that is occurring in the system. A large $f'.R'$ coupled with R_{b0} being nearly equal to R_m suggests that significant cake layer was formed.

Furthermore, the ratio of φ by $K\alpha$, which indicates to a fair degree the distribution density of blocked pores area (i.e., an indication of pore blocking), is just over twice the size of pore constriction parameter β (as roughly 1.42 is superior to roughly 0.64). This indicates that pore blocking mechanism was predominant during fouling. Consequently, the majority of the fouling was controlled by both pore blocking and cake filtration.

Figure 5 shows the normalised volumetric flow rate ratios plotted against the filtration time at constant TMP of 45 kPa, for MLSS concentrations of 6.32 and 7.24 g/L for the square-shaped SMBR model; with the solid lines representing the best fit simulation solutions. Data collected show a colossal drop in flux of over 72% for both MLSS levels. This is within expectation based on past studies [24].

Also, as can be seen, the best fit curve at this high TMP is extremely poor (especially after 80 minutes). However, again the fouling curve's trend is of the right magnitude and in the right direction to allow an analysis of the fouling behaviour that is occurring. Superficially, analysis would suggest that fouling may be due to all three fouling mechanisms, but it can be argued that fouling was primarily dominated by cake filtration and pore blocking mechanisms.

A relatively big $f'.R'$, R_m being nearly equal to R_{b0} coupled with similar sized cake removal factor, g_0, and blocked pore area constant, k_{Ab}, all strongly shows that a big cake layer was formed (see Table 2). However, with the pore blocking parameter, α, being roughly twice as big as the pore constriction parameter, β, it can be inferred that the pore blocking mechanism was also prevalent

 doi:10.20944/preprints201806.0187.v1

during fouling. Hence, the bulk of the fouling was dominated by both cake filtration and pore blocking mechanisms.

In terms of comparison, overall both SMBR fouling models gave a near identical depiction of the fouling mechanisms that occurred during filtration processes. Although their point-to-point experimental data fits were poor, the trend of their simulated fouling curves more than made up for this deficit.

4. Conclusions

In the study conducted by Paul and Jones [23] using a novel RMBR (Avanti's RPU-185), they created a fouling model incorporating rotational effects as well as hydrodynamics. Their study concluded that rotation efficiency in terms of fouling prevention was estimated to be 12%. In their follow up study, they developed a static fouling model based on the RMBR fouling model by switching off its rotating functions. The work showed that a rotating MBR system could increase flux throughput by a significant amount when compared against a similar static system although there are obvious additional capital and operational cost implications [24].

In this research work, a standard fouling model for a SMBR that included hydrodynamics was developed using the viscosity to mixed liquor relationship model developed by Yang et al. [22]. It was fed filtration data collected at high TMP and MLSS concentrations from running the bespoke square-shaped SMBR. Although point-to-point experimental data fitting was poor, the trend of the simulated curve (i.e. fouling decline) was respectable. This is to be expected since at high MLSS levels biological activities vary wildly. When compared with the SMBR model that was obtained by switching off the rotational functions of the RMBR model, the latter has better point-to-point experimental data fitting but shares similar and respectable fouling curve fitting trends with the former.

Overall, despite the discrepancies in point-to-point data fitting of both SMBR models, their similar fouling decline curve fitting trends suggest that respectable agreement was reached between experimental and simulated fouling decline (and by extension occurrence of fouling mechanisms). This not only indicates that the basic premise of the developed RMBR model was sound in empirical terms when compared to a standard flux model, but also vindicates the usage of a complex RMBR model. Follow on studies will now compare results from the RMBR system using rotational models developed by other researchers to ascertain the effectiveness rotating MBR modelling approach.

Author Contributions: Conceptualization, P.Paul.; Methodology, P.Paul.; Software, F.Jones.; Validation, F.Jones.; Formal Analysis, F.Jones.; Investigation, P.Paul. and F.Jones; Resources, P.Paul.; Data Curation, F.Jones.; Writing-Original Draft Preparation, F.Jones.; Writing-Review & Editing, P.Paul.; Visualization, F.Jones.; Supervision, P.Paul.; Project Administration, P.Paul.; Funding Acquisition, P.Paul.

Funding: This research was funded by a Research Grant of The Royal Society, UK.

Acknowledgments: The authors would like to acknowledge Avanti Technology, USA, for their technical contribution and The Royal Society, UK, for providing funding to allow this work to proceed.

Conflicts of Interest: The authors declare no conflict of interest. The funders had no role in the design of the study; in the collection, analyses, or interpretation of data; in the writing of the manuscript, and in the decision to publish the results.

Preprints (www.preprints.org) | NOT PEER-REVIEWED | Posted: 12 June 2018 doi:10.20944/preprints201806.0187.v1

Nomenclature

Symbols

A, remaining membrane area available for permeate (m^2);
A_0, (total) membrane area (m^2);
A_b, blocked membrane area (m^2);
A_u, unblocked membrane area (m^2);
A_{u0}, initial unblocked area (m^2);
C_b, liquid bulk concentration (g/L);
C_{MLSS}, mixed liquor suspended solids concentration (g/L);
f', fraction of foulants contributing to particles deposit growth (−);
g_0, cake removal factor (−),
J_0, initial filtrate flux of clean membrane ($m\ s^{-1}$);
J_{m0}, initial total flux within membrane ($m\ s^{-1}$);
J_u, unblocked flux ($m\ s^{-1}$);
k_{Ab}, k_{A_b} area constant parameter for blocked pores (−);
K_α, area distribution density (m^{-1});
PT, transmembrane pressure at membrane periphery (Pa);
Q_0, initial volumetric flow rate ($m^3\ s^{-1}$);
Q_t, total volumetric flow rate ($m^3\ s^{-1}$);
R', unit cake layer thickness per unit mass of fluid filtered (m/kg);
R'_c, specific cake resistance (m^{-2});
R_b, resistance of solids deposit over a region of membrane (m^{-1});
R_{b0}, initial resistance of solids deposit (m^{-1});
$R_{in,b}$, membrane's resistance & resistance from pore constriction (m^{-1});
R_m, clean membrane's resistance (m^{-1});
R_{total}, total membrane resistance (m^{-1});
t, filtration time (s);
t_b, time at which a membrane region was first blocked (s);

Greek Letters

α, pore blockage parameter (m^2/kg);
α_v, air scouring coefficient (-);
β, pore constriction parameter (kg);
δ', is the resistance distribution factor of cake layer (m^{-1});
θ_c, cake's depth or thickness (m);
μ, viscosity (Pa s);
φ, a constant accounting for total amount of cake layers formed (−);

References

References should be numbered in order of appearance and indicated by a numeral or numerals in square brackets, e.g., [1] or [2,3], or [4–6]. See the end of the document for further details on references.

1. Templeton, M. R.; Butler, D. *Introduction to Wastewater Treatment*. Ventus Publishing ApS. 2011.

2. Jeppsson, U. Modelling aspects of wastewater treatment processes. MSc dissertation. Lund University, Industrial Electrical Engineering and Automation (IEA), Lund Institute of Technology (LTH). IEA, LTH, Box 118, SE-221 00 Lund, Sweden. 1996.
3. Gernaey, K.; van Loosdrecht, M.; Henze, M.; Lind, M.; Jørgensen, S. Activated sludge wastewater treatment plant modelling and simulation: state of the art. *Env. Mod. & Software* **2004**, *19(9)*, 763–783.
4. Xing, C. H.; Tardieu, E.; Qian, Y.; Wen, X. H. Ultrafiltration membrane bioreactor for urban wastewater reclamation. *J. Membr. Sci.* **2000**, *177*, 73-82.
5. Fenu, A.; Guglielmi, G.; Jimenez, J.; Sperandio, M.; Saroj, D.; Lesjean, B. Activated sludge model (ASM) based modelling of membrane bioreactor (MBR) processes: A critical review with special regard to MBR specificities. *Water Res* **2010**, *44*, 4272- 4294.
6. Chang, I.S.; Le Clech, P.; Jefferson, B.; Judd, S. Membrane Fouling in Membrane Bioreactors for Wastewater Treatment. *J. Env. Eng*. **2002**, 1018-1029.
7. Zuthi, M.F.R.; Ngo, H.H.; Guo, W.S. Modelling bioprocesses and membrane fouling in membrane bioreactor (MBR): A review towards finding an integrated model framework. *Biores. Tech.* **2012**, *122*, 119–129.
8. Bentzen, T. R.; Ratkovich, N.; Madsen, S.; Jensen, J. C.; Bak, S. N.; Rasmussen, M. R. Analytical and numerical modelling of Newtonian and non-Newtonian liquid in a rotational cross-flow MBR. *Water Sci. Tech*. **2012**, *66(11)*, 2318-2327.
9. Bhattacharjee, C.; Bhattacharya, P.K. Ultrafiltration of black liquor using rotating disk membrane module. *Sep. & Pur. Tech*. **2005**, *49*, 281–290.
10. Jaffrin, M.Y.; Ding, L.H.; Akoum, O.; Brou, A. A hydrodynamic comparison between rotating disk and vibratory dynamic filtration systems. *J. Membr. Sci.* **2004**, *242*, 155–167.
11. Jørgensen, M.K.; Malene, T.P.; Morten, L.C. Dependence of shear and concentration on fouling in a membrane bioreactor with rotating membrane discs. *AIChE J* **2014**, *60*, 706–715.
12. Judd, S. *The MBR Book: Principles and Applications of Membrane Bioreactors*, 1st ed.; Elsevier: Amsterdam, Netherlands. 2006.
13. Drews, A. Membrane fouling in membrane bioreactors - characterization, contradiction, causes and cures. *J. Membr. Sci.* **2010**, *363(1)*, 1–28.
14. Ahn, Y.T.; Choi, Y.K.; Jeong, H.S.; Shin, S.R. Modeling of extracellular polymeric substances and soluble microbial products production in a submerged MBR at various SRTs. *Water Sci. Tech.* **2006**, *53*, 209–216.
15. Rosenberger, S.; Laabs, C.; Lesjean, B.; Gnirss, R.; Amy, G.; Jekel, M.; Schrotter, J.C. Impact of colloidal and soluble organic material on membrane performance in membrane bioreactors for municipal wastewater treatment. *Water Res.* **2006**, *40*, 710–720.
16. Hermia, J. Constant pressure blocking filtration laws-application to power-law non-Newtonian fluids. *Trans. IChemE*. **1982**, *60a*, 183-187.
17. Yoon, S.-H. *Membrane Bioreactor Processes: Principles and Applications*. CRC Press. 2015.
18. Meng, F.; Zhang, H.; Li, Y.; Zhang, X.; Yang, F. Application of fractal permeation model to investigate membrane fouling in membrane bioreactor. *J. Membr. Sci.* **2005**, *262*, 107–116.
19. Liu, R.; Huang, X.; Sun, Y.F.; Qian, Y. Hydrodynamic effect on sludge accumulation over membrane surfaces in a submerged membrane bioreactor. *Process Biochem.* **2003**, *39*, 157-163.
20. Duclos-Orsello, C.; Li, W.; Hob, C. A three mechanism model to describe fouling of microfiltration membranes. *J. Membr. Sci.* **2006**, *280*, 856–866.
21. Paul, P. Development and Testing of a Fully Adaptable Membrane Bioreactor Fouling Model for a Sidestream Configuration System. *Membranes* **2013**, *3(2)*, 24-43.
22. Yang, F.; Bick, A.; Shandalov, S.; Brenner, A.; Oron, G. Yield stress and rheological characteristics of activated sludge in an airlift membrane bioreactor. *J. Membr. Sci.* **2009**, *334*, 83–90.
23. Paul, P.; Jones, F. A. Development of a comprehensive fouling model for a novel rotating membrane bioreactor system, *Water* **2015**, *7(2)*, 377-397.
24. Paul, P.; Jones, F. A. Advanced Wastewater Treatment Engineering – Investigating Membrane Fouling in both Rotational and Static Membrane Bioreactor Systems Using Empirical Modelling. I*nt. J. Environ. Res. Public Health* **2016**, *13(1)*, 100.
25. Liang, S.; Song, L.; Tao, G.; Kekre, K.A.; Seah, H. A modeling study of fouling development in membrane bioreactors for wastewater treatment. *Water Environ. Res.* **2006**, *78*, 857–863.

 doi:10.20944/preprints201806.0187.v1

448 26. Le Clech, P.; Jefferson, B.; Chang, I.S.; Judd, S.J. Critical flux determination by the flux-step method in a
449 submerged membrane bioreactor. *J. Membr. Sci.* **2003**, 227, 81–93.

450